Volume 52 | Number 44 | 4 June 2016 | Pages 7055–7174

ChemComm

Chemical Communications

www.rsc.org/chemcomm

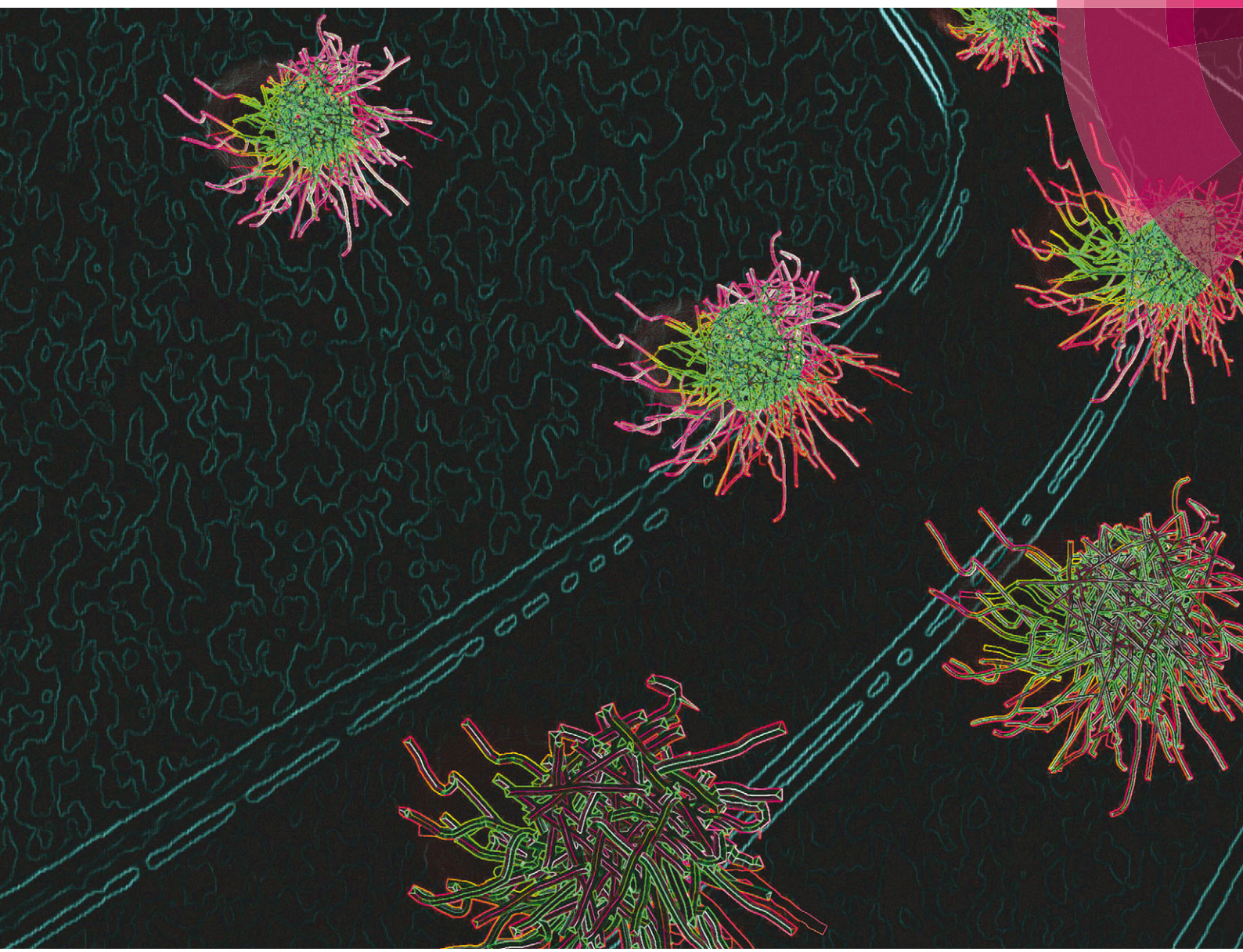

ISSN 1359-7345

ROYAL SOCIETY OF CHEMISTRY

COMMUNICATION

Xiupeng Wang *et al.*

Rod-shaped and fluorine-substituted hydroxyapatite free of molecular immunopotentiators stimulates anti-cancer immunity *in vivo*

175 YEARS

ChemComm

COMMUNICATION

View Article Online
View Journal | View Issue

Cite this: *Chem. Commun.*, 2016, 52, 7078

Received 6th April 2016,
Accepted 19th April 2016

DOI: 10.1039/c6cc02848a

www.rsc.org/chemcomm

Rod-shaped and fluorine-substituted hydroxyapatite free of molecular immunopotentiators stimulates anti-cancer immunity *in vivo*†

Xiupeng Wang,*[a] Xia Li,[a] Atsuo Ito,[a] Yohei Watanabe[b] and Noriko M. Tsuji[b]

Herein, rod-shaped and fluorine-substituted hydroxyapatite nanoparticles (FHA) were synthesized using a facile hydrothermal method. The rod-shaped FHA significantly increased the cellular uptake of a model antigen by bone marrow dentritic cells *in vitro*, improved antigen presentation *in vivo*, stimulated immune-related cytokine secretion *in vitro* and *ex vivo*, and enhanced the anti-cancer immunity *in vivo*.

A significant challenge in vaccine development is the synthesis of a proper adjuvant.[1] An adjuvant, an indispensable part of a vaccine, enhances the magnitude, breadth, quality and longevity of specific immune responses, and reduces the amount of antigen needed for immunization.[2–10] However, as the most commonly used adjuvant in human vaccine, the aluminum compounds (alum) work only with certain diseases.[11] Alum provokes Th2 immune responses, although a Th1 immune response is required in anti-cancer immunity.[12]

Therefore, the development of an adjuvant capable of stimulating robust Th1 anti-cancer immunity is crucial for cancer immunotherapy. Generally, a human adjuvant should be safe, stable, inexpensive, biodegradable, capable of antigen delivery, and act as an immunopotentiator.[13,14] Although some studies have proved that hydroxyapatite (HA) is safe, stable, inexpensive, biodegradable and capable of biomolecule delivery,[15–21] far fewer reports have examined HA as an adjuvant in cancer immunotherapy.[22,23] Herein, for the first time, we proved that rod-shaped and fluorine-substituted hydroxyapatite (FHA) nanoparticles free of molecular immunopotentiators can act as immunoadjuvants in cancer immunotherapy, as the FHA nanoparticles significantly increased cellular uptake of a model antigen *in vitro*, improved antigen presentation *in vivo*, promoted immune-related cytokine secretion *in vitro* and *ex vivo*, and enhanced the anti-cancer immunity *in vivo* (Fig. 1).

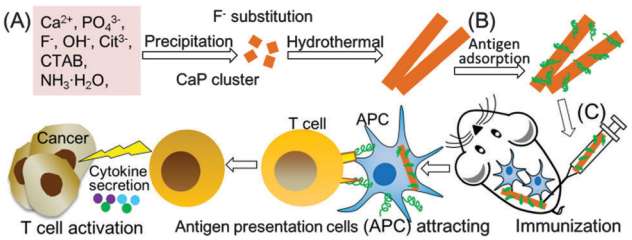

Fig. 1 Schematic illustration of synthesis (A), antigen adsorption (B), and the immunoadjuvant effect in cancer immunotherapy (C) of rod-shaped FHA.

The rod-shaped FHA nanoparticles were synthesized using a simple hydrothermal method (Fig. 1A). Typically, 3 mmol of $Ca(NO_3)_2$, 0.5 g of hexadecyltrimethylammonium bromide (CTAB), 10 mL of ammonia solution ($NH_3{\cdot}H_2O$), 6 mmol of trisodium citrate, 0.67 mmol of NaF, 2 mmol of $(NH_4)_2HPO_4$ and 60 mL of ultrapure water were hydrothermally treated at 180 °C for 24 h. The product was collected, separated by centrifugation, and washed with ultrapure water and ethanol in sequence. Then, the obtained product was re-dispersed in 150 mL of 6 g L^{-1} NH_4NO_3 in ethanol and stirred at 60 °C for 1 h to remove the template CTAB. The product was separated by centrifugation, washed with ultra-pure water several times, and freeze-dried to obtain the final FHA nanoparticles. HA nanoparticles were synthesized using the same method as FHA, without the addition of NaF.

SEM and TEM images showed that the FHA nanoparticles were rod-shaped, with a uniform width of about 20 nm and a length of about 300 nm (Fig. 2A–C). No extra diffraction peaks attributed to impurity phases appeared in the XRD patterns of FHA nanoparticles (JCPDS No. 15-876, Fig. 2D). FHA nanoparticles showed no IR-absorption bands for the OH-group at 3470 and 630 cm^{-1}, indicating the substitution of F^- for OH^- in the HA crystal lattice. No absorption bands for CTAB were

[a] *Health Research Institute, Department of Life Science and Biotechnology, National Institute of Advanced Industrial Science and Technology (AIST), Central 6, 1-1-1 Higashi, Tsukuba, Ibaraki 305-8566, Japan. E-mail: xp-wang@aist.go.jp*

[b] *Immune Homeostasis Lab., Biomedical Research Institute, Department of Life Science and Biotechnology, National Institute of Advanced Industrial Science and Technology (AIST), Central 6, 1-1-1 Higashi, Tsukuba, Ibaraki 305-8566, Japan*

† Electronic supplementary information (ESI) available: Experimental section. See DOI: 10.1039/c6cc02848a

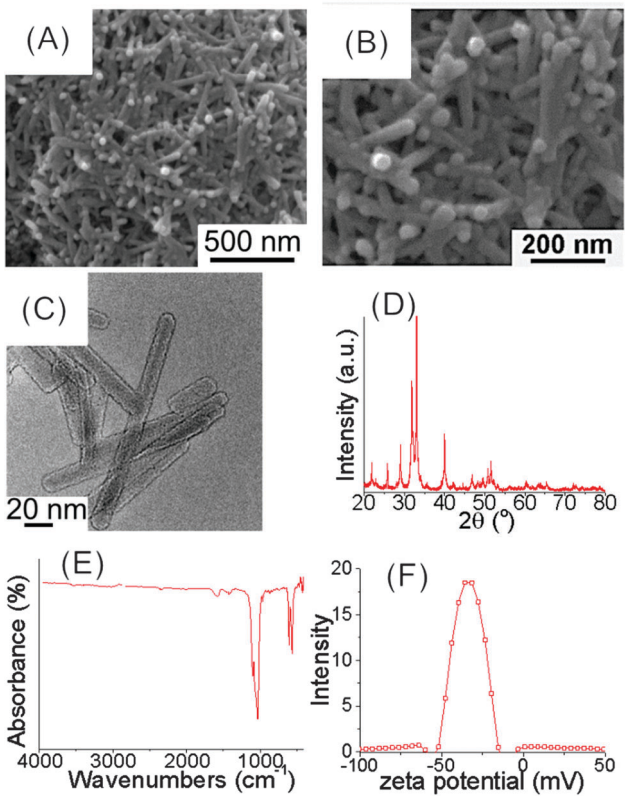

Fig. 2 Physicochemical characterization of rod-shaped FHA nanoparticles. SEM (A and B) and TEM (C) images, XRD pattern (D), FTIR spectrum (E), zeta potential in PBS(−) (F).

observed in the FTIR spectra, indicating the complete removal of the template by the NH_4NO_3-ethanol solution (Fig. 2E). The zeta potential of FHA nanoparticles was around −33.6 mV in PBS(−) (Fig. 2F). The negative zeta potential below −30 mV implies that the FHA nanoparticles can be well dispersed and stable against aggregation in solution. HA nanoparticles showed a very similar XRD pattern and surface charge as compared with FHA, but the length of HA is only about 100 nm.[10]

To evaluate the effect of particles on the cellular uptake of antigen, fluorescein conjugates of ovalbumin (F-OVA, a model antigen) loaded onto particles were cultured with bone marrow dentritic cells (BMDCs) for 4 h *in vitro*, respectively. Alum loaded with F-OVA and free F-OVA were used as controls. The amount of F-OVA internalized by the BMDCs was tested after washing twice with PBS(−). Interestingly, the amount of F-OVA internalized by BMDCs strongly depended on the adjuvant. BMDCs cultured with FHA-F-OVA and HA-F-OVA showed 17.2 and 13.2 times the F-OVA uptake compared to those with free F-OVA, respectively (Fig. 3B). Moreover, BMDCs cultured with FHA-F-OVA showed significantly increased F-OVA uptake compared with those with HA-F-OVA. In contrast, BMDCs cultured with alum-F-OVA showed only 1.9 times the F-OVA uptake of those with free F-OVA. The cellular uptake of F-OVA by BMDCs was further confirmed by confocal microscopy images. Free F-OVA was slightly engulfed by BMDCs after 4 h (Fig. 3C1–C4). In contrast, FHA nanoparticles loaded with F-OVA were efficiently engulfed by BMDCs after 4 h (Fig. 3D1–D4).

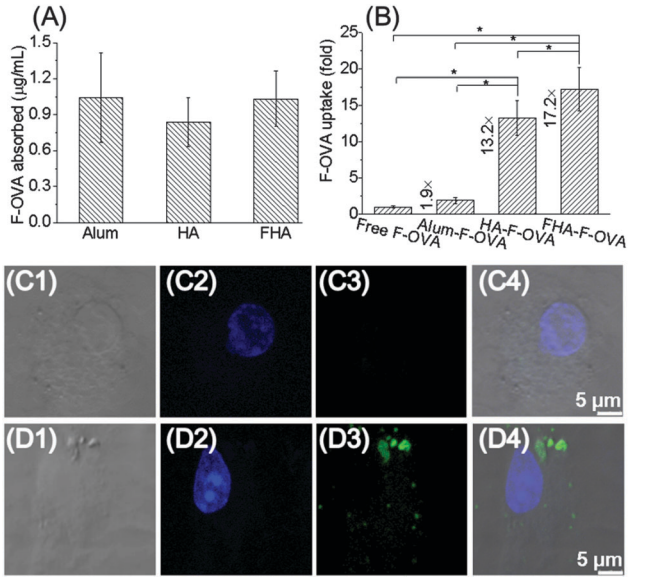

Fig. 3 Rod-shaped HA and FHA nanoparticles adsorbed F-OVA (A), and promoted cellular uptake of F-OVA by BMDCs *in vitro*; quantitative result of F-OVA cellular uptake (B), representative confocal laser scanning microscopy images after cell exposure to free F-OVA (C1–C4) and FHA-F-OVA (D1–D4): bright field cell images (C1 and D1), cell nucleus (C2 and D2), F-OVA (C3 and D3), merged images (C4 and D4). (n = 8, *p < 0.05).

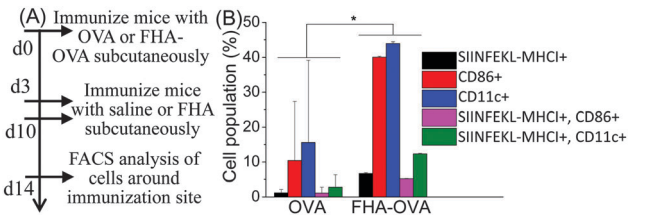

Fig. 4 Rod-shaped FHA nanoparticles promote DCs accumulation and cross-presentation of SIINFEKL-MHCI with DCs around injection site *in vivo*. Experimental treatment protocol (A), cell population (B). (n = 3, *p < 0.05).

The effect of FHA nanoparticles on antigen-presenting cell accumulation and cross-presentation of SIINFEKL-MHCI with antigen-presenting cells was studied. Cells around the immunization site were harvested and tested by flow cytometry, 14 days after the first immunization (Fig. 4A). From the results, FHA-OVA significantly improved DCs ($CD86^+$, and $CD11C^+$) accumulation and antigen presentation ($SIINFEKL\text{-}MHCI^+$) compared with free OVA around the immunization site. Moreover, FHA-OVA significantly improved cross-presentation of SIINFEKL-MHCI with DCs than free OVA (Fig. 4B and Fig. S5, ESI†).

The rod-shaped morphology of FHA nanoparticles is favorable for the efficient antigen cellular uptake. The particle size and shape are very important parameters to control the non-specific cellular uptake and subsequent cellular responses. Mesoporous silica particles with a long-rod-shaped morphology were taken up in larger amounts and faster internalization rates than those with a short-rod-shaped or round-shaped morphology.[24] Subsequently, the efficient cellular uptake of FHA nanoparticles will be beneficial for the delivery of the adsorbed antigen to

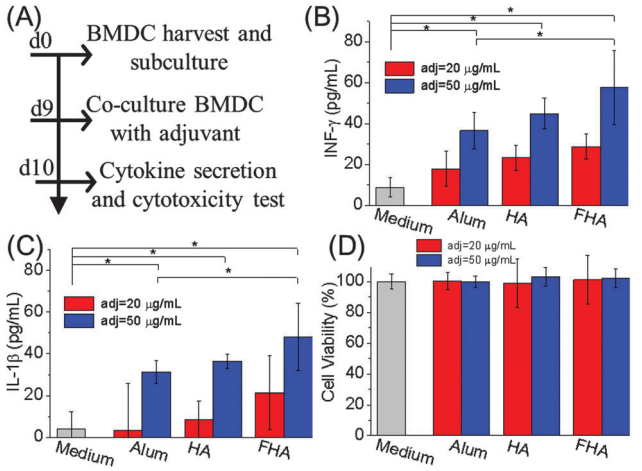

Fig. 5 Rod-shaped FHA nanoparticles stimulate immunogenic activity without detectable cytotoxicity. Experimental protocol (A), rod-shaped FHA nanoparticles stimulate IFN-γ (B) and IL-1β (C) secretion by BMDCs *in vitro*. Rod-shaped FHA nanoparticles showed no cytotoxicity (D). (n = 6, $*p < 0.05$).

immune cells and the stimulation of the immune responses. The uptake of antigens by the immune cell is the first step that eventually leads to a specific immune response.[25,26] Maximizing the efficiency of antigen presentation is considered to be the key point for the successful development of a therapeutic immune response.[27]

In vitro immunogenic activity and cytotoxicity of rod-shaped HA and FHA nanoparticles were evaluated by culturing the nanoparticles with BMDCs (Fig. 5A). BMDCs cultured with FHA showed the highest interferon-γ (IFN-γ) and interleukin-1β (IL-1β) secretion among all the samples. At 50 μg mL^{-1} of particle concentration, BMDCs cultured with FHA showed significantly enhanced IFN-γ and IL-1β secretion compared to those cultured with alum and medium (Fig. 5B and C). Rod-shaped FHA showed no cytotoxicity at 20–50 μg mL^{-1} as tested by BMDCs (Fig. 5D). Moreover, rod-shaped FHA nanoparticles showed no obvious cytotoxicity at 5–50 μg mL^{-1} as tested by cell viability and lactate dehydrogenase (LDH) cytotoxicity of NIH3T3 cells (Fig. S1 and S2, ESI†).

Anti-cancer immunity of the rod-shaped FHA nanoparticles was tested using mouse lymphoma E.G7-OVA cells (Fig. 6A). Mice immunized with alum-OVA and without immunization showed obvious tumor growth 4w after E.G7-OVA challenge (Fig. 6B, red circle). In contrast, FHA-OVA immunized mice showed significantly smaller tumor size than those immunized with alum-OVA or without immunization (Fig. 6B). Percentage of mice without cancer or with cancer smaller than 15 mm for FHA-OVA, Alum-OVA and saline injected mice 4w after E. G7-OVA challenge was 60%, 20% and 0%, respectively (Fig. 6C). The cancer volume of FHA-OVA, Alum-OVA and saline injected mice 4w after E.G7-OVA challenge was 1573 ± 969, 4221 ± 2845 and 7013 ± 2866 mm^3, respectively (Fig. 6D). Similarly, mice immunized by an established Th1-biased control adjuvant (poly IC)[28,29] markedly inhibited cancer challenge (Fig. 6E). In addition, the anti-cancer effect was not due to non-specific cytotoxicity of FHA, as FHA without antigen OVA did not show any anti-cancer response (Fig. 6F).

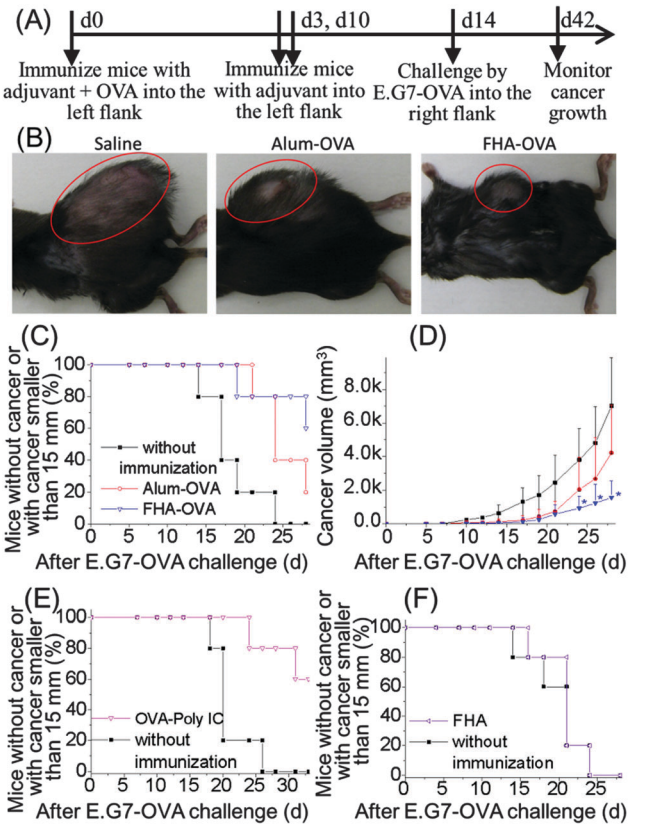

Fig. 6 Rod-shaped FHA nanoparticles exhibit anti-cancer immunity *in vivo*. Experimental protocol (A), typical cancer photos of mice 4w after E.G7-OVA challenge (B), mice without cancer or with cancer smaller than 15 mm (C, E and F), cancer volume of mice after E.G7-OVA challenge (D). (n = 5, $*p < 0.05$).

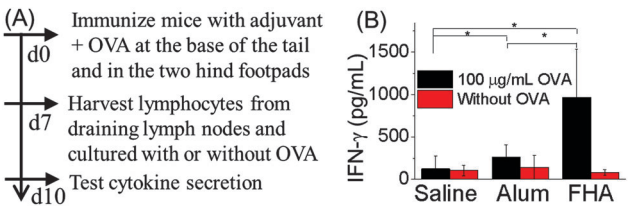

Fig. 7 Rod-shaped FHA nanoparticles induce OVA-specific IFN-γ secretion highly related to anti-cancer immunity by lymphocytes after 3 d of culture *ex vivo*. Experimental treatment protocol (A), IFN-γ secretion (B). (n = 3 × 2, $*p < 0.05$).

To further clarify the mechanism of the anti-cancer immunity of the rod-shaped FHA nanoparticles, the immune related cytokine secretion from the lymphocytes was studied (Fig. 7A). The rod-shaped FHA nanoparticles significantly improved OVA-specific IFN-γ secretion by lymphocytes than alum adjuvant and without adjuvant groups *ex vivo*. Mice treated with the rod-shaped FHA nanoparticles showed maximum IFN-γ secretion at 969 ± 567 pg mL^{-1}, when stimulated by 100 μg mL^{-1} OVA *ex vivo* (Fig. 7B). IFN-γ is a cytokine critical for innate and adaptive immunity, which has immunoregulatory and anti-cancer properties, and can direct cytotoxic effects on cancer cells in conjunction with the cancer necrosis factor.[30] Moreover, IFN-γ is a key cytokine

that stimulates innate immune responses and directs adaptive T cell response toward the Th1 type. Th1 immunity is very important for cancer immunotherapy, as patients with advanced cancer often have impaired cell-mediated immunity associated with a switch from Th1 to Th2.[31]

Besides, safety is another key requirement for a successful adjuvant. Since rod-shaped FHA nanoparticles showed no obvious cytotoxicity, the FHA nanoparticles are a good candidate for an adjuvant.

To conclude, FHA nanoparticles with rod-shaped morphology were synthesized using a simple hydrothermal method. For the first time, we showed that the rod-shaped FHA nanoparticles significantly improve the cellular uptake of a model antigen *in vitro*, improved antigen presentation *in vivo*, and improved immune related cytokine secretion *in vitro* and *ex vivo*. Most importantly, the rod-shaped FHA nanoparticles free of molecular immunopotentiators markedly inhibited cancer challenge *in vivo*. The proposed rod-shaped FHA nanoparticles are promising for an immunoadjuvant in cancer immunotherapy.

We thank Dr Yu Sogo and Ms Kazuko Yoshiyuki at AIST, Dr Tadao Ohno at the Nippon Dental University for their advice and technical assistance in ELISA analysis and animal experiments. This study was supported in part by KAKENHI (Grant-in-Aid for Young Scientists B, No. 26750162 and 23700567) and the NIMS Molecule & Material Synthesis Platform in ''Nanotechnology Platform Project'' operated by the Ministry of Education, Culture, Sports, Science and Technology (MEXT), Japan.

Notes and references

1 P. Marrack, A. S. Mckee and M. W. Munks, *Nat. Rev. Immunol.*, 2009, **9**, 287–293.
2 X. P. Wang, X. Li, A. Ito, N. M. Tsuji, Y. Sogo, Y. Watanabe and T. Ohno, *Angew. Chem., Int. Ed.*, 2016, **55**, 1899–1903.
3 X. P. Wang, X. Li, K. Yoshiyuki, Y. Watanabe, Y. Sogo, T. Ohno, N. M. Tsuji and A. Ito, *Adv. Healthcare Mater.*, 2016, DOI: 10.1002/adhm.201501013.
4 A. Wack and R. Rappuoli, *Curr. Opin. Immunol.*, 2005, **17**, 411–418.
5 X. P. Wang, X. Li, A. Ito, Y. Sogo and T. Ohno, *Acta Biomater.*, 2013, **9**, 7480–7849.
6 X. P. Wang, X. Li, A. Ito, Y. Sogo and T. Ohno, *J. Biomed. Mater. Res., Part A*, 2014, **102**, 967–974.
7 X. P. Wang, X. Li, Y. Sogo and A. Ito, *RSC Adv.*, 2013, **3**, 8164–8167.
8 X. P. Wang, X. Li, K. Onuma, Y. Sogo, T. Ohno and A. Ito, *Sci. Rep.*, 2013, **3**, 2203.
9 X. Li, X. P. Wang, Y. Sogo, T. Ohno, K. Onuma and A. Ito, *Adv. Healthcare Mater.*, 2013, **2**, 863–871.
10 X. P. Wang, X. Li, A. Ito, Y. Watanabe, Y. Sogo, M. Hirose, T. Ohno and N. M. Tsuji, *Colloids Surf., B*, 2016, **139**, 10–16.
11 H. Ren, Q. X. Zhang, L. Qie and G. L. Baker, *ACS Symp. Ser.*, 2013, **1150**, 3–21.
12 J. M. Brewer, M. Conacher, C. A. Hunter, M. Mohrs, F. Brombacher and J. Alexander, *J. Immunol.*, 1999, **163**, 6448–6454.
13 D. T. O'Hagan and E. De Gregorio, *Drug Discovery Today*, 2009, **14**, 541–551.
14 A. Pashine, N. M. Valiante and J. B. Ulmer, *Nat. Med.*, 2005, **11**, s63–s68.
15 X. Li, X. P. Wang, A. Ito, Y. Sogo, K. Cheng and A. Oyane, *Mater. Sci. Eng., C*, 2009, **29**, 216–221.
16 X. P. Wang, A. Ito, Y. Sogo, X. Li and A. Oyane, *Acta Biomater.*, 2010, **6**, 962–968.
17 X. P. Wang, A. Ito, Y. Sogo, X. Li and A. Oyane, *J. Biomed. Mater. Res., Part A*, 2010, **92**, 1181–1189.
18 X. P. Wang, A. Ito, Y. Sogo, X. Li, H. Tsurushima and A. Oyane, *Acta Biomater.*, 2009, **5**, 2647–2656.
19 X. P. Wang, A. Oyane, H. Tsurushima, Y. Sogo, X. Li and A. Ito, *Biomed. Mater.*, 2011, **6**, 045004.
20 X. P. Wang, F. P. He, X. Li, A. Ito, Y. Sogo, O. Maruyama, R. Kosaka and J. D. Ye, *Sci. Technol. Adv. Mater.*, 2013, **14**, 035002.
21 X. P. Wang, A. Ito, X. Li, Y. Sogo and A. Oyane, *Biofabrication*, 2011, **3**, 022001.
22 D. R. Ciocca, P. Frayssinet and F. D. Cuello-Carrion, *Cell Stress Chaperones*, 2007, **12**, 33–43.
23 M. Abei, T. Okumura, K. Fukuda, T. Hashimoto, M. Araki, K. Ishige, I. Hyodo, A. Kanemoto, H. Numajiri, M. Mizumoto, T. Sakae, H. Sakurai, J. Zenkoh, G. Ariungerel, Y. Sogo, A. Ito, T. Ohno and K. Tsuboi, *Radiat. Oncol.*, 2013, **8**, 239.
24 X. L. Huang, X. Teng, D. Chen, F. Q. Tang and J. Q. He, *Biomaterials*, 2010, **31**, 438–448.
25 M. W. Hess, M. G. Schwendinger, E. L. Eskelinen, K. Pfaller, M. Pavelka, M. P. Dierich and W. M. Prodinger, *Blood*, 2000, **95**, 2617–2623.
26 S. Y. Chang, H. J. Ko and M. N. Kweon, *Exp. Mol. Med.*, 2014, **46**, e84.
27 H. Y. Li, Y. H. Li, J. Jiao and H. M. Hu, *Nat. Nanotechnol.*, 2011, **6**, 645–650.
28 O. Schulz, S. S. Diebold, M. Chen, T. I. Naslund, M. A. Nolte, L. Alexopoulou, Y. T. Azuma, R. A. Flavell, P. Liljestrom and C. R. E. Sousa, *Nature*, 2005, **433**, 887–892.
29 X. Chuai, H. Chen, W. Wang, Y. Deng, B. Wen, L. Ruan and W. Tan, *PLoS One*, 2013, **8**, e54126.
30 J. R. Schoenborn and C. B. Wilson, *Adv. Immunol.*, 2007, **96**, 41–101.
31 M. R. Shurin, L. Lu, P. Kalinski, A. M. Stewart-Akers and M. T. Lotze, *Springer Semin. Immunopathol.*, 1999, **21**, 339–359.